

3-D reconstruction of the inner heliosphere from remote-sensing data: A global solar wind boundary that includes CME transient effects

H.-S. Yu, B. V. Jackson, P. P. Hick, A. Buffington, J. M. Clover, and M. Tokumaru

Citation: [AIP Conference Proceedings](#) **1500**, 147 (2012); doi: 10.1063/1.4768758

View online: <http://dx.doi.org/10.1063/1.4768758>

View Table of Contents: <http://scitation.aip.org/content/aip/proceeding/aipcp/1500?ver=pdfcov>

Published by the [AIP Publishing](#)

Articles you may be interested in

[3D Reconstruction of Density Enhancements Behind Interplanetary Shocks from Solar Mass Ejection Imager White-Light Observations](#)

AIP Conf. Proc. **1216**, 659 (2010); 10.1063/1.3395953

[Large-Scale Heliospheric Structure during Solar-Minimum Conditions using a 3D Time-Dependent Reconstruction Solar-Wind Model and STELab IPS Observations](#)

AIP Conf. Proc. **1216**, 355 (2010); 10.1063/1.3395873

[Molecular Spectroscopy and Remote-Sensing of the Earth's Atmosphere: Progress from Laboratory Studies](#)

AIP Conf. Proc. **1100**, 143 (2009); 10.1063/1.3116934

[Time-dependent tomography of hemispheric features using interplanetary scintillation \(IPS\) remote-sensing observations](#)

AIP Conf. Proc. **679**, 75 (2003); 10.1063/1.1618545

[Remote sensing measurements of the corona with the Solar Probe](#)

AIP Conf. Proc. **385**, 77 (1997); 10.1063/1.51769

3-D Reconstruction of the Inner Heliosphere From Remote-Sensing Data: A Global Solar Wind Boundary That Includes CME Transient Effects

H.-S. Yu^a, B.V. Jackson^a, P.P. Hick^a, A. Buffington^a, J.M. Clover^a,
and M. Tokumaru^b

^aCASS, UCSD, La Jolla, CA, USA; ^bSTELab, Nagoya University, Nagoya, Japan

Abstract. At UCSD, remote-sensing analyses of the inner heliosphere have been regularly carried out using interplanetary scintillation (IPS) data for almost two decades. These analyses have measured and reconstructed 3D solar wind structure throughout this time period. These global results, especially using Solar-Terrestrial Environment Laboratory (STELab) IPS observations, provide time-dependent density and velocity that is nearly complete over the whole heliosphere for the major part of each year and with a time cadence of about one day. When using the volumetric velocity from this time-dependent tomography, we can accurately convect solar surface magnetic fields outward and thus provide values of the magnetic field throughout the global volume. We can extract a "boundary" at any height in the inner heliosphere from this analysis. These extrapolations also allow us to trace the magnetic connection of any heliospheric location back to the inner boundary surface as an approximation to the propagation path of the solar energetic particles. Here we present sample determinations of these global solar wind boundaries from recent IPS data, and provide some of the details that allow the interpolation of these boundary values across the STELab data "outage" periods.

Keywords: Solar Wind; CMEs; MHD

PACS: 96.50.Ci; 96.60.Ph; 95.30.Qd

1. INTRODUCTION

Interplanetary Scintillation (IPS) observations have long been used to remotely-sense small-scale (100-200km) heliospheric density variations in the solar wind crossing the line of sight (LOS) to a point radio source [1, 2]. These density inhomogeneities disturb the signal from point radio sources producing intensity variations, that, on Earth's surface, cause a projected pattern travelling away from the Sun with the solar wind speed. This pattern, measured and correlated between different radio sites, allows a determination of the solar wind outflow speed. The 'normalized scintillation level' (*g*-level) of IPS radio source signal relative to a nominal average allows a determination of the solar wind density. A greater variation in *g*-level amplitude generally means a higher density along the line of sight.

A time-dependent 3D tomographic reconstruction technique, has been developed at the University of California, San Diego (UCSD) over the years [3-6]. This Computer-Assisted Tomography (CAT) technique allows solar wind temporal variations to be

mapped in three spatial dimensions over time and provides a 3D reconstruction of transient heliospheric structures such as coronal mass ejections (CMEs) as well as co-rotating features. We have implemented our CAT program using the Solar-Terrestrial Environment Laboratory (STELab), Japan, IPS velocity and scintillation level data from 1999 onward to determine heliospheric structures in real time at periods when STELab data were available (generally from May through December each year up until 2010). In 2011, STELab IPS g -level data became available on a year around basis. When using our tomographic IPS velocity, we can also convect solar surface magnetic fields outward [7], and thus provide magnetic field values throughout the global volume. These reconstructed heliospheric density, velocity, and vector magnetic fields are available from 15 solar radii out to 3.0 AU.

Section 2. describes our technique for fitting STELab IPS velocity and g -level data and compares our results with a CME event observed on 9 November 2011. This section also describes the analysis we use to provide extrapolated magnetic field in the heliosphere. We present sample determinations of the global solar wind boundaries for 3D-MHD models from recent IPS data in Section 3., and provide some details that allow the interpolation of these boundary values across the STELab "outage" periods. The summary and discussion are in Section 4.

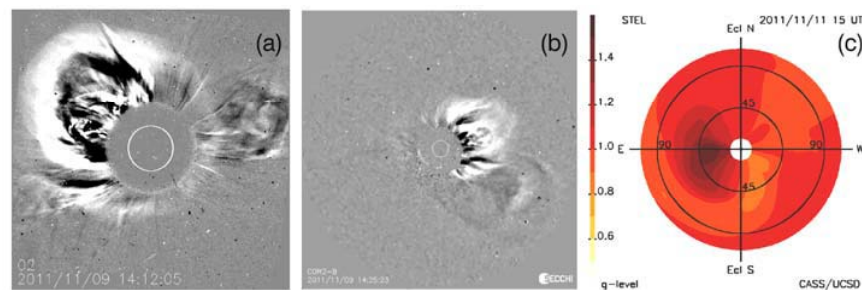


FIGURE 1. Coronagraph images of (a) LASCO C2 at 14:12 UT and (b) STEREO COR2 at 14:25 UT. (c) g -level "fish-eye" map based on the IPS 3D reconstruction. This figure is reprinted from [8].

2. TIME-DEPENDENT 3D TOMOGRAPHY ANALYSIS

The details of the mathematical and computational method of the UCSD time-dependent 3D-reconstruction technique can be found in Hick and Jackson [3], and Jackson *et al.* [9]. Jackson *et al.* [6, 10, 11], and Kojima *et al.* [12] give a more general summary of these analyses, and the computer methods used in the 3D reconstructions. The early analyses assume that the heliosphere co-rotates with the Sun. In more recent work [4, 5, 13] the co-rotating assumption has been relaxed to allow the outward motion of heliospheric structures and their changed weighting along the line of sight to provide global 3D reconstructions over time. Our technique incorporates a purely kinematic solar wind model. The LOS segment 3D weights are projected back in space and time to a solar wind inner boundary (the "source surface") that is usually set at 15 solar radii. A fully 3D solar wind model least-squares fit to the observations is derived by assuming radial outflow and enforcing conservation of mass and mass flux [10]. If the 3D solar wind model does not match the overall observations, the boundary conditions are iteratively adjusted to minimize the differences between

modeled and observed IPS g -level and velocity. The inner boundary Carrington maps of velocity and density are smoothed at each iteration using a 2D Gaussian spatial and temporal filter. Locations in the model that are unaffected by this iterative procedure (and thus undetermined) usually remain unfilled in the final result.

Since the spring of 2011, we have extended our analyses to include available *in-situ* measurements of velocity [14], and density [8] into our real-time forecast analyses. This extension more accurately reproduces and forecasts the real-time Advanced Composition Explorer (ACE) *in-situ* density and velocity measurements at Earth at the appropriate spatial and temporal resolutions of the 3D reconstructions.

As an example of these analyses, at 13:36UT on 9 November 2011 there was a halo CME [15] observed by the Solar and Heliospheric Observatory (SOHO) Large Angle and Spectrometric CORonagraph (LASCO) C2 and C3 instruments [16]. Figure 1 shows this CME, or rather the CME sequence, as in the coronagraph and later in the IPS 3D reconstructions on 11 November. In this CME sequence, a slightly earlier CME moves outward to the southeast and more towards the Earth, while a more-dominant CME in the LASCO C2 field of view travels rapidly to the solar northeast and is more distant from the Earth (Fig. 1a). The Solar TERrestrial RELations Observatory-behind Earth orbit spacecraft (STEREO-B) [17] observes a density enhancement that peaks at about 10 Np at 18:00 UT on 11 November and another at about 06 UT on 12 November (Fig. 1b). Our IPS fisheye map (Fig. 1c) displays these CMEs heading to the east of the Sun-Earth line (see also [8]). Figure 2 shows a density (2a) and a velocity (2b) time series comparison between IPS tomography and ACE data for this CME sequence. Our density and velocity reconstructions show good agreement with the ACE *in-situ* data at 1AU.

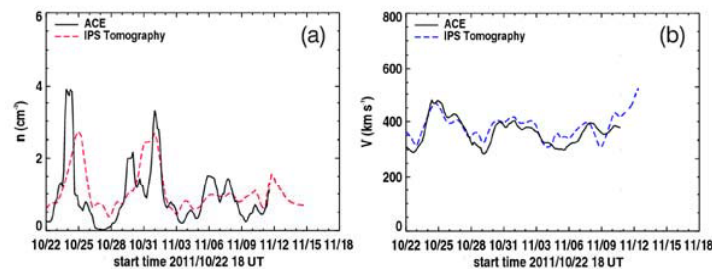


FIGURE 2. (a) Density and (b) velocity time series extraction from the time-dependent 3D reconstruction using STELab IPS data during the 11 November 2011 event period compared with ACE Level-0 $\frac{3}{4}$ -day averaged data. The dashed-line time series in each plot is the reconstruction result, and the solid line corresponds to the ACE *in-situ* measurements which stop at 16:00 UT on 11 November. The IPS tomography continues as forecast for another 3 days. Panel (a) is reprinted from [8].

From the density ecliptic cut (Fig. 3a) of IPS 3D reconstruction at 15:00UT on 11 November, we can see a small density enhancement along the Sun-Earth line associated with the oncoming halo CME and far more material moving outward to the east of the Sun-Earth line [8]. For some space weather effects, especially at Earth, the magnetic field directions of the transient heliospheric structures are important in determining how an interaction with planetary magnetic fields will proceed. In 2005, the Current Sheet Source Surface (CSSS) potential magnetic field model [18] was introduced into our tomography analysis [7] as an extension of the kinematic model.

The CSSS model provides a radial magnetic field with realistic amplitudes that are updated as frequently as one day at the inner source surface of our tomographic analysis. The potential field model provides only long-term (several-day) changes in the radial magnetic field at the source surface. We extrapolate this magnetic field upward (by forward modeling) to all locations within the 3D matrix using the IPS tomographic velocity [7]. Thus, our extrapolation provides only radial and tangential heliographic magnetic field components from the rotation of the source surface below any specific location within the global volume. The analysis from our modeling allows an immediate location and a track of any remote heliospheric position to the inner boundary surface in order to estimate possible solar high energetic particle propagation paths as shown in Fig. 3.

For use as a continuous boundary for global or 3D-MHD modeling, an attempt is made to interpolate between all outages and areas unfilled by the tomographic reconstructions. The IPS analyses are provided by daily measurements from STELab, when radio sources are overhead, generally from ~ 50 radio sources that measure g -level and perhaps ~ 10 that measure velocity. While there have been notable exceptions such as the “Bastille_Day CME” in the year 2000, and the “Halloween Storm CME” in 2003, the fastest CMEs can be missed on any given day at STELab, and only the heliospheric aftermath of fast CME events viewed. Jackson *et al.* [8, 13] provide additional discussion about the IPS and STELab data outages. Short-term outages and unfilled regions are interpolated from nearest neighbors in time and space. For longer outages, the tomographic analysis fills the data set assuming the heliosphere co-rotates. With the inclusion of *in-situ* densities and velocities near Earth, the co-rotational analysis dominates when only *in-situ* data are available. In the case where there are no remotely-sensed IPS measurements that fill the heliospheric polar regions, these regions are filled by extrapolation from the regions surrounding the solar poles.

3. GLOBAL SOLAR WIND BOUNDARY

The resulting global parameters of density, velocity, and vector magnetic field derived by the UCSD 3D reconstructions have been compared successfully with *in-situ* measurements obtained near Earth, STEREO, Mars, Venus, MESSENGER, and at the Ulysses spacecraft [13, 15, 19-21]. These same global results can be provided as a time-dependent lower boundary for use in 3D-MHD models.

We can provide these synoptic boundary maps in many different coordinate frames, and here show latitude and longitude in Inertial Heliographic coordinates (IHG) from our analysis. Figure 4a-4d respectively show density, velocity, radial and tangential magnetic field synoptic maps in latitude and longitude at 0.25 AU in IHG coordinates at 15:00 UT on 11 November 2011. We map our boundaries to 0.25AU because it is here that remotely-sensed IPS measurements generally provide the maximum response along the line of sight, and because some 3D-MHD models [22] are better equipped to extrapolate outward from this solar distance. The Earth location in 3.31° N, 333° at 1 AU (\oplus) and its projection at 0.25 AU in 3.31° N, 12.1° (\odot) are marked on these maps showing the structures present at this projection location. Figure 4a shows a density enhancement at the east of the Sun-Earth line as observed by the STEREO-B spacecraft. Following the 9 November halo CME, there was evidence of a small shock

that we assume is associated with this event at $\sim 06:00$ UT on 12 November that has an associated increase in density observed by the Charge, Element, Isotope Analysis System (CELIAS) Proton Monitor [23] near Earth. The hourly-averaged ACE level-2 solar energetic particle flux plot also shows a strong increase of flux starting around 11 November (Fig. 4e). The density and velocity synoptic maps at 0.25 AU (Figure 4a,b) show a relatively dense and high speed structure near the Earth projected location along the potential propagation path of the solar energetic particles.

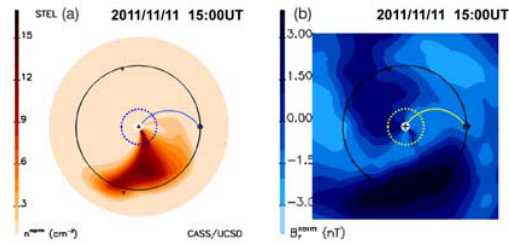


FIGURE 3. (a) Density and (b) radial magnetic field ecliptic cut from the 3D reconstruction of the 9 November 2011 CMEs. The Sun is centered in these plots with the Earth marked (\oplus) on its orbit that is indicated by the circle in the plots. The dashed circle shows the inner boundary at 0.25 AU and the solid Sun to Earth line shows the convection trace.

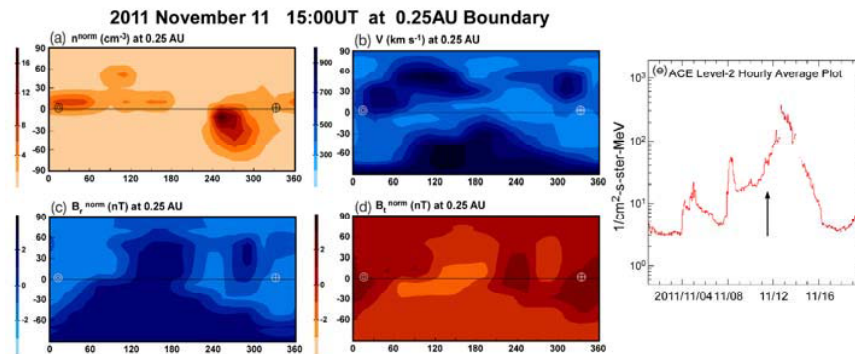


FIGURE 4. Global solar wind boundaries of (a) density, (b) velocity, (c) radial and (d) tangential magnetic field at 0.25 AU and (e) ACE level-2 hourly-averaged solar energetic particle flux during the 11 November 2011 event period. See the text for the discussion in detail.

4. SUMMARY AND DISCUSSION

The analysis of IPS data provides low-resolution global heliospheric measurements of density and velocity with a time cadence of one day, and slightly longer cadences for some magnetic field components. How data outages are handled in these analyses is important, and specific to each period studied, and the application of the analysis. For current specific applications it is best to certify that there are high-quality data (both remotely-sensed and *in situ*) available for the periods of study. This is especially true when using these analyses as a lower boundary for 3D-MHD forward-modeling techniques. For archival data, more than one *in-situ* data set (and not only that from ACE) is available near Earth for use in these analyses.

There are several sources of heliospheric remote sensing data (IPS, SMEI), but the most long-term and substantiated source (that also measures velocity globally) is IPS data from the STELab arrays in Japan. Accurate observations of inner heliosphere parameters coupled with the best physics can extrapolate these outward to Earth or the interstellar boundary. We note that currently, this procedure only works at Earth to provide a smooth transition from *in-situ* measurements to those remotely-sensed and, while there should be an improvement at all the inner planets using this procedure, this cannot be tested and certified unless there are plasma monitors at these locations that measure the values *in situ*.

ACKNOWLEDGMENTS

H.-S. Yu, B.V. Jackson, P.P. Hick, A. Buffington, and J.M. Clover were supported at UCSD by NSF grants ATM-0852246, and AGS-1053766, NASA grant NNX11AB50G and by AFOSR grant FA9550-11-1-0324. The authors wish to acknowledge and thank the group at STELab, Nagoya University not included in the author list (M. Kojima, K. Fujiki, and students) for their continued support, and for making IPS data sets available under the auspices of a joint collaborative agreement between the Center for Astrophysics and Space Sciences at UCSD and STELab, Nagoya University. We also wish to thank Kevin Schenk and the LASCO coronagraph group for the 9 November 2011 halo CME images taken using the C2 coronagraph, and also to the STEREO SECCHI group for making available their COR2 images.

REFERENCES

1. A. Hewish, *et al.*, *Nature* **203**, 1214-1217 (1964).
2. S. Ananthkrishnan, *et al.*, *Journal of Geophysical Research* **85**, 6025-6030 (1980).
3. P. P. Hick and B. V. Jackson, in *Society of Photo-Optical Instrumentation Engineers (SPIE) Conference Series*, edited by S. Fineschi and M. A. Gummin (2004), Vol. 5171, pp. 287-297.
4. B. V. Jackson, *et al.*, in *Solar Wind Ten*, edited by M. Velli, R. Bruno and F. Malara (2003), Vol. 679, pp. 75-78.
5. B. V. Jackson and P. P. Hick, in *Astrophysics and Space Science Library*, edited by D. E. Gary and C. U. Keller (2004), Vol. 314, pp. 355.
6. B. V. Jackson, *et al.*, *Journal of Atmospheric and Solar-Terrestrial Physics* **73**, 1214-1227 (2011).
7. T. Dunn, *et al.*, *Solar Physics* **227**, 339-353 (2005).
8. B. V. Jackson, *et al.*, *Solar Physics* (**in press**) (2012).
9. B. V. Jackson, *et al.*, *Advances in Geosciences* **21**, 339 (2010).
10. B. V. Jackson, *et al.*, *Journal of Geophysical Research* **103**, 12049-12068 (1998).
11. B. V. Jackson, *et al.*, *Journal of Geophysical Research (Space Physics)* **113** (2008).
12. M. Kojima, *et al.*, *Journal of Geophysical Research* **103**, 1981-1990 (1998).
13. B. V. Jackson, *et al.*, *Advances in Geosciences* (**in press**) (2012).
14. B. V. Jackson, *et al.*, *Solar Physics* **265**, 245-256 (2010).
15. K. Schenk, in *10 November Soho-halo-alert*, 111109 (2011).
16. G. E. Brueckner, *et al.*, *Solar Physics* **162**, 357-402 (1995).
17. M. L. Kaiser, *et al.*, *Space Science Reviews* **136**, 5-16 (2008).
18. X. Zhao and J. T. Hoeksema, *Journal of Geophysical Research* **100**, 19-33 (1995).
19. B. V. Jackson, *et al.*, in *11th Annual IAC* (2012).
20. M. M. Bisi, *et al.*, *Advances in Geosciences* **14**, 161 (2009).
21. M. M. Bisi, *et al.*, *Advances in Geosciences* **21**, 33 (2010).
22. N. V. Pogorelov, *et al.*, *Space Science Reviews* **143**, 31-42 (2009).
23. D. Hovestadt, *et al.*, *Solar Physics* **162**, 441-481 (1995).